

# Biocatalytic Synthesis of a Novel Bioactive Ginsenoside Using UDP-Glycosyltransferase from *Bacillus Subtilis* 168

Yumei Hu <sup>1,2</sup>, Hao Li <sup>2</sup>, Yingying Qu <sup>2</sup>, Xiao Zhang <sup>2</sup>, Juankun Zhang <sup>1</sup>, and Longhai Dai <sup>2,\*</sup>

<sup>1</sup> Tianjin Key Laboratory of Industrial Microbiology, College of Biotechnology, Tianjin University of Science and Technology, Tianjin 300457, China; hu\_ym@tib.cas.cn (Y.H.); zhangjk@tust.edu.cn (J.Z.)

<sup>2</sup> State Key Laboratory of Biocatalysis and Enzyme Engineering, Hubei Collaborative Innovation Center for Green Transformation of Bio-Resources, Hubei Key Laboratory of Industrial Biotechnology, School of Life Sciences, Hubei University, Wuhan 430062, China; Li\_Hao\_4312@126.com (H.L.); chiuyy@126.com (Y.Q.); zhangxiao\_hubu@126.com (X.Z.)

\* Correspondence: dailonghai@hubu.edu.cn

Received: 11 February 2020; Accepted: 25 February 2020; Published: 3 March 2020

**Abstract:** Ginsenoside Rg3 is a bioactive compound from *Panax ginseng* and exhibits diverse notable biological properties. Glycosylation catalyzed by uridine diphosphate-dependent glycosyltransferase (UGT) is the final biosynthetic step of ginsenoside Rg3 and determines its diverse pharmacological activities. In the present study, promiscuous UGT Bs-YjiC from *Bacillus subtilis* 168 was expressed in *Escherichia coli* and purified via one-step nickel chelate affinity chromatography. The in vitro glycosylation reaction demonstrated Bs-YjiC could selectively glycosylate the C12 hydroxyl group of ginsenoside Rg3 to synthesize an unnatural ginsenoside Rd12. Ginsenoside Rd12 was about 40-fold more water-soluble than that of ginsenoside Rg3 (90  $\mu$ M). Furthermore, in vitro cytotoxicity of ginsenoside Rd12 against diverse cancer cells was much stronger than that of ginsenoside Rg3. Our studies report the UGT-catalyzed synthesis of unnatural ginsenoside Rd12 for the first time. Ginsenoside Rd12 with antiproliferative activity might be further exploited as a potential anticancer drug.

**Keywords:** ginsenoside Rg3; unnatural ginsenoside; glycosyltransferase; water solubility; antiproliferative activity

## 1. Introduction

Ginseng (*Panax ginseng*) is the most famous medicinal-edible plant recorded in the Chinese Pharmacopoeia [1,2]. This precious perennial herb is crowned the “King of All Herbs” [3]. Ginseng has been widely used to provide nutrition, strengthen immunity, and increase vital energy for thousands of years in Oriental countries [4]. Ginsenosides are the principal effective ingredients of ginseng [5]. These natural compounds are a group of glycosylated triterpene saponins and exhibit diverse intriguing pharmacological activities, including anti-inflammatory, antiaging, anticancer, antitumor, neuroprotective, skin-whitening, and immunoregulatory effects [6–9].

Over 140 ginsenosides have been isolated from diverse *Panax* species [10]. These naturally occurring products are mainly grouped into protopanaxadiol-type (PPD) and protopanaxatriol-type (PPT) according to the structure of the aglycone skeleton [11]. Glycosylation catalyzed by uridine diphosphate-dependent glycosyltransferase (UGT) is the last biosynthetic step of ginsenosides and determines their tremendous structural and functional diversity [12]. PPD contains hydroxyl groups at C3, C12, and C20 positions, whereas PPT contains hydroxyl groups at C3, C6, C12, and C20 positions. For PPD-type ginsenosides, the sugar moieties are attached to the C3 and/or C20 hydroxyl groups. For PPT-type ginsenosides, the sugar moieties are attached to the C6 and/or C20 hydroxyl

groups. Despite both PPD and PPT skeletons containing the C12 hydroxyl group, ginsenosides with sugar moieties attached to the C12 hydroxyl group have never been identified from *Panax* species.

Compared with plant-derived UGTs, microbial UGTs generally exhibit remarkable aglycone flexibility and poor regiospecificity [13–18]. These promiscuous UGTs could be exploited as robust biocatalysts for glycodiversification of natural and unnatural products for new drug discovery [19,20]. Bs-YjiC from *Bacillus subtilis* 168 is a flexible and effective UGT toward a numerous number of structurally diverse compounds [21,22]. Bs-YjiC could glucosylate the C3, C6, and C12 hydroxyl groups of PPT to synthesize unnatural ginsenosides [10]. Bs-YjiC could also catalyze a continuous two-step glucosylation of the C3 and C12 hydroxyl groups of PPD to synthesize ginsenoside Rh2 and an unnatural ginsenoside F12 [23]. However, the regiospecificity of Bs-YjiC toward other ginsenosides have not been thoroughly elucidated.

In the present study, Bs-YjiC was heterologously expressed in *Escherichia coli* and purified to homogeneity via one-step nickel chelate affinity chromatography. Ginsenoside Rg3 (a PPD-type ginsenoside) was selected as the aglycone using uridine diphosphate glucose (UDPG) as the glucosy donor (Figure 1). Furthermore, water solubility and antiproliferative activity of the synthesized unnatural ginsenoside toward diverse cancer cell lines were also determined.

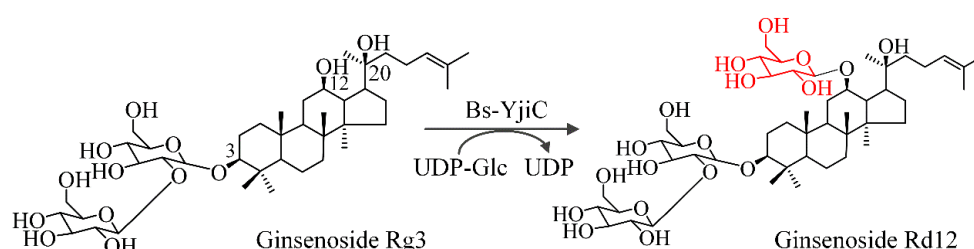


**Figure 1.** Chemical structures of ginsenosides Rg3 and Rd12.

## 2. Results and Discussion

### 2.1. Expression and Purification of Bs-YjiC

Bs-YjiC was cloned from *B. subtilis* 168 and heterologously expressed in *E. coli* BL21 (DE3) as an N-terminal His<sub>6</sub>-tagged protein. Recombinant Bs-YjiC was mainly expressed as a soluble protein and could be purified easily by one-step nickel chelate affinity chromatography. SDS-PAGE analysis indicated a clear band at around 45 kDa (over 90% purity), which was consistent with the calculated molecular weight of the recombinant Bs-YjiC (Figure 2).

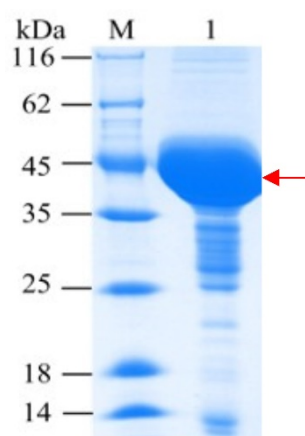


**Figure 2.** SDS-PAGE analysis of purified Bs-YjiC. M: Protein marker; 1: Purified Bs-YjiC.

## 2.2. Glycosylation of Ginsenoside Rg3 with Bs-YjiC

Glycosyltransferase activity of Bs-YjiC toward ginsenoside Rg3 was determined with UDPG as the glucosyl donor. High-performance liquid chromatography (HPLC) analysis of the Bs-YjiC-catalyzed reaction mixtures revealed that only one new product with the retention time (RT) of 13.1 min was produced, whereas no new product was detected in the control reactant (Figure 3A). Further, HPLC coupled with ionization-mass spectrometry (HPLC-ESI-MS) analysis of the new product ( $[M+H]^+$   $m/z \sim 947.5585$ ,  $[M+H-H_2O]^+$   $m/z \sim 929.5475$ ,  $[M+H-Glc-H_2O]^+$   $m/z \sim 767.4908$ ,  $[M+H-2Glc-H_2O]^+$   $m/z \sim 605.4396$ , and  $[M+H-3Glc-2H_2O]^+$   $m/z \sim 425.3783$ ) demonstrated one glucosyl moiety was attached to ginsenoside Rg3 (calculated molecular weight,  $[M+H]^+$   $m/z \sim 785.5061$ ) (Figure 3B).

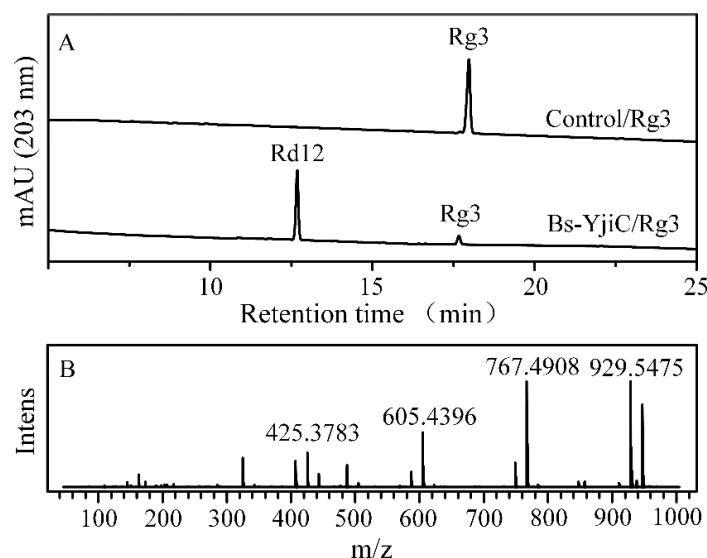


**Figure 3.** HPLC-ESI-MS analysis of the reactants of ginsenoside Rg3. (A) HPLC chromatograms of the reaction mixtures. (B) MS spectra for ginsenoside Rd12.

The newly synthesized product was purified by preparative HPLC and its structure was elucidated by nuclear magnetic resonance (NMR) spectroscopy, including  $^1H$  NMR,  $^{13}C$  NMR, homonuclear correlation spectroscopy (COSY), heteronuclear multiple-bond correlation spectroscopy (HMBC), and heteronuclear singular quantum correlation (HSQC) (Figures S1–S5). The  $^1H$  and  $^{13}C$  NMR spectra of the new product was similar to that of ginsenoside Rg3 [24], except for an additional glucosyl moiety (Table 1). Three anomeric proton signals ( $\delta_H$  4.4–4.7 ppm) in  $^1H$  NMR spectra and three anomeric carbon signals ( $\delta_C$  100.5–105.4 ppm) in the  $^{13}C$  NMR spectra suggested that the PPD skeleton was decorated with three glucosyl moieties. The significant downfield shift at  $\delta_C$  79.39 (~9 ppm, C12, 'glycosylation shift'), as well as the correlations between the glucosyl moiety anomeric signal  $H'''$  ( $\delta_H$  4.53 ppm, d,  $J = 8.0$  Hz) and C12 ( $\delta_C$  79.39 ppm) in the HMBC spectra, revealed that the C12 hydroxyl group of ginsenoside Rg3 was decorated with a glucosyl moiety [22]. In addition, the anomeric proton-coupling constant ( $J = 8.0$  Hz) indicated that the C12 glucosyl moiety of ginsenoside Rg3 adopted the  $\beta$ -configuration, which was in agreement with the inverting mechanism of UGTs [25]. Thus, this ginsenoside Rg3-derived unnatural product was 3-O- $\beta$ -D-glucopyranosyl-(1-2)-O- $\beta$ -D-glucopyranosyl-12-O- $\beta$ -D-glucopyranosyl-protopanaxadiol (an unnatural PPD-type ginsenoside named ginsenoside Rd12 in this study).

Kinetic analysis of Bs-YjiC toward ginsenoside Rg3 revealed that the  $K_m$  value was 99.0  $\mu M$ , which was comparable to many previously reported UGTs involved in the biosynthesis of different triterpene saponins [13,25,26]. The turnover number ( $k_{cat}$ ) of Bs-YjiC was 5.2  $s^{-1}$ , which was much higher than that of ginseng-derived UGTs (Figure S6) [11,27]. Thus, the catalytic efficiency ( $k_{cat}/K_m$ ,  $5.3 \times 10^4 s^{-1} M^{-1}$ ) of Bs-YjiC toward ginsenoside Rg3 was considerably high. These results suggested that Bs-YjiC was an effective UGT for enzymatic glycosylation of ginsenoside Rg3. Glycosylation

mediated by UGTs is the final biosynthetic step and the key bottleneck of ginsenosides [24]. A chassis cell that can accumulate considerable number of ginsenoside Rg3 has been constructed [24,28], it would be of great interest to produce unnatural ginsenoside Rd12 by introduction of Bs-YjC into the ginsenoside Rg3-producing yeast cell factories.

**Table 1.**  $^1\text{H}$ - and  $^{13}\text{C}$ -NMR spectral of unnatural ginsenoside Rd12 (methanol- $d_4$ , 600 MHz).

C	$\delta_{\text{C}}$ (ppm)	$\delta_{\text{H}}$ (ppm)
1	36.69	1.44 (1H, m), 1.59 (1H, m)
2	27.61	1.37 (1H, m), 1.67 (1H, m)
3	91.26	3.23 (1H, br.s)
4	40.56	-
5	57.48	0.79 (1H, m)
6	19.19	1.41 (1H, m), 1.47 (1H, m)
7	36.69	1.36 (1H, m), 1.47 (1H, m)
8	38.12	-
9	53.15	1.69 (1H, overlapped)
10	41.94	-
11	31.86	1.80 (1H, m), 2.04 (1H, m)
12	79.39	3.92 (1H, m)
13	47.30	1.10 (1H, m)
14	54.96	-
15	28.65	1.26 (1H, m), 1.38 (1H, m)
16	28.36	1.43 (1H, m), 2.03 (1H, m)
17	51.14	-
18	17.44	0.98 (3H, s)
19	16.74	0.96 (3H, s)
20	74.72	-
21	26.21	1.15 (3H, s)
22	35.75	1.32 (2H, m)
23	23.28	1.18 (2H, m), 1.67 (1H, m)
24	126.30	5.17 (1H, tr)
25	131.80	-
26	25.92	1.71 (3H, s)
27	17.77	1.65 (3H, s)
28	27.61	1.10 (3H, s)
29	16.71	0.89 (3H, s)
30	16.21	1.07 (3H, s)
C3-O-inner-Glc-1'	105.38	4.47 (1H, d, $J = 8.0$ Hz)
2'	81.11	3.60 (m)
3'	77.59	3.38 (1H, overlapped)
4'	71.55	3.13 (1H, overlapped)
5'	78.26	3.27 (1H, m)
6'	62.82	3.69 (1H, dd, $J = 7.8, 4.2$ Hz); 3.86 (1H, overlapped)
C3-O-outer-Glc-1''	104.50	4.70 (1H, d, $J = 8.0$ Hz)
2''	76.27	3.14 (m)
3''	77.81	3.38 (1H, overlapped)
4''	70.92	3.36 (1H, overlapped)
5''	78.33	3.24 (1H, m)
6''	62.36	3.69 (1H, dd, $J = 7.8, 4.2$ Hz); 3.86 (1H, overlapped)
C12-O-inner-Glc-1'''	100.53	4.53 (1H, d, $J = 8.0$ Hz)
2'''	75.08	3.13 (m)
3'''	77.96	3.14 (1H, overlapped)
4'''	71.86	3.20 (1H, overlapped)
5'''	78.44	3.60 (1H, m)
6'''	63.08	3.67 (1H, dd, $J = 8.4, 3.0$ Hz); 3.81 (1H, overlapped)

Note: Glc: Glucosyl moiety; ppm: Parts per million.

### 2.3. Aqueous Solubility of Ginsenoside Rd12

The poor aqueous solubility of natural products resulted in a low absorption and a short retention time in the intestine [21]. Glycosylation mediated by UGTs transfers the hydrophilic sugar moieties to natural products, which can significantly enhance their solubility and thus improve their bioavailability and pharmacodynamics [29,30]. The aqueous solubility of ginsenoside Rg3 was limited to 90  $\mu\text{M}$ . However, the aqueous solubility of unnatural ginsenoside Rd12 increased to 3.6 mM, which was 40-fold more water-soluble than that of ginsenoside Rg3.

### 2.4. In Vitro Cytotoxicity of Ginsenoside Rd12

Glycosylation contributes to the tremendous structural and functional diversity of ginsenosides [10]. Thus, the antiproliferative activity of unnatural ginsenoside R12 toward colon cancer cells Lovo, gastric cancer cell line SNU719, and lung cancer cell line DMS53 was evaluated using ginsenoside Rg3 as the positive control. Ginsenoside Rg3 exhibited poor inhibition toward colon cancer cells Lovo and lung cancer cells DMS53 with  $\text{IC}_{50}$  values exceeding 400  $\mu\text{M}$ , whereas  $\text{IC}_{50}$  values of unnatural ginsenoside Rd12 toward colon cancer cells Lovo and lung cancer cells DMS53 were 40.7 and 46.4  $\mu\text{M}$ , respectively (Table 2). The  $\text{IC}_{50}$  values of ginsenosides Rg3 and Rd12 toward gastric cancer cell SNU719 cells were 359.4 and 112.2  $\mu\text{M}$ , respectively. These results suggested that the attachment of a glucosyl moiety to the C12 hydroxyl group of ginsenoside Rd12 enhanced its antiproliferative activity toward colon cancer cells Lovo, gastric cancer cell line SNU719, and lung cancer cell line DMS5.

**Table 2.** In vitro cytotoxicity of ginsenoside Rd12 ( $\mu\text{M}$ )

Compound	Lovo <sup>1</sup>	DMS53 <sup>2</sup>	SNU719 <sup>3</sup>
Rg3	>400	>400	359.4 $\pm$ 30.1
Rd12	40.7 $\pm$ 5.9	46.4 $\pm$ 4.1	112.2 $\pm$ 11.9

<sup>1</sup> Lovo: Colon cancer cells; <sup>2</sup> DMS53: Lung cancer cells; <sup>3</sup> SNU719: Gastric carcinoma cells.

## 3. Materials and Methods

### 3.1. Chemicals, Reagents, and Cancer Cell Lines

Ginsenoside Rg3 was purchased from Biopurify Phytochemicals (Chengdu, Sichuan, China). UDP-glucose (UDPG), dimethyl sulfoxide (DMSO), methanol, deuterated methanol (methanol-*d*<sub>4</sub>), acetonitrile, and thiazolyl blue tetrazolium bromide (MTT) agent were obtained from Sigma-Aldrich (St. Louis, MO, USA). The colon cancer cells Lovo, lung cancer cells DMS53, and gastric cancer cells SNU719 were obtained from CoBioer Biosciences (Nanjing, China). Dulbecco's modified Eagle's medium, streptomycin, and penicillin were obtained from Gibco (Haverhill, MA, USA).

### 3.2. Heterologous Expression and Enzymatic Activity of Bs-YjiC

Bs-YjiC (GenBank No. NP\_389104) was subcloned into plasmid pET28a and recombinant Bs-YjiC was prepared as described previously [10]. Enzymatic assay (0.5 mL) of Bs-YjiC was conducted with 50 mM Tris-HCl (pH 8.0), 10 mM UDPG, 2 mM ginsenoside Rg3, and 5  $\mu\text{g}$  Bs-YjiC at 40 °C for 10 min. Reactants adding total lysate protein from *E. coli* BL21 (DE3) expressing pET28a was used as the control. The reaction mixtures were quenched by the addition of equal volume of chromatographic-grade methanol. After centrifugation at 12,000 g for 5 min, the reactants were monitored by HPLC and HPLC-ESI-MS as described previously [24].

### 3.3. Kinetic Parameters of Bs-YjiC toward Ginsenoside Rg3

Kinetic studies of Bs-YjiC toward ginsenoside Rg3 were carried out in 300  $\mu\text{L}$  volumes (50 mM Tris-HCl (pH 8.0), 10 mM UDPG, and a variable concentration of ginsenoside Rg3 [50–600  $\mu\text{M}$ ]). The reactants were precultured at 40 °C for 20 min and initiated by the addition of 0.5  $\mu\text{g}$  Bs-YjiC.

Subsequently, the reaction mixtures were incubated at 40 °C for 10 min and stopped by the addition of equal volume of chromatography-grade methanol. Finally, the samples were analyzed by HPLC as described above.

### 3.4. Water Solubility Determination

Water solubility of ginsenosides Rd12 and Rg3 was determined as described previously [31]. An amount of 5 mg ginsenosides Rd12 and Rg3 were dissolved in 0.4 mL double-distilled water, respectively. The samples were mixed by ultrasonication for 1 h. Subsequently, the samples were maintained at 25 °C for 2 h. After centrifugation at 15,000 g for 10 min, the aliquots were analyzed directly by HPLC mentioned above.

### 3.5. Cell Viability Assay

Antiproliferative activity of ginsenosides Rd12 and Rg3 against colon cancer cells Lovo, gastric cancer cell line SNU719, and lung cancer cell line DMS5 was performed as described previously [23]. The cancer cells were seeded into the 96-well plates with a density of  $1 \times 10^5$  cells/mL and incubated for 24 h. Subsequently, the cancer cell lines were incubated with variable concentrations of ginsenosides Rd12 and Rg3 for another 48 h. MTT solution (15  $\mu$ L, 5 mg/mL) was added to the wells and the cancer cell lines were incubated for 4 h. Finally, the medium was removed and DMSO (150  $\mu$ L) was added into the plates. The samples were measured spectrophotometrically by an ELISA spectrophotometer at 570 nm.

### 3.6. HPLC and HPLC-ESI-MS Analysis of the Glycosylated Product

An Agilent 1260 HPLC system equipped with a C18 column was applied to analyze the samples as described previously [23]. The column was eluted with phase A (double-distilled water/0.1% formic acid, v/v) and phase B (chromatography-grade acetonitrile/0.1% formic acid, v/v). The flow rate was 1 mL/min with a gradient program of 25–85% B in 0–25 min. HPLC-ESI-MS analysis was operated in positive ion mode and full scan (50–1500 Da) as described previously [25].

### 3.7. Structural Elucidation of Ginsenoside Rd12 by NMR Spectroscopy

A scale-up reaction (100 mL) was conducted for the preparation of unnatural ginsenoside Rd12. Ginsenoside Rd12 was purified by an Agilent 1260 preparative HPLC system as described previously [23]. The preparative column was eluted with double-distilled water (phase A) and chromatography-grade methanol (phase B) using a flow rate of 10 mL/min and a gradient of 25–100% phase B in 0–60 min. Subsequently, the fractions containing purified ginsenoside Rd12 were collected and concentrated by reduced pressure distillation. After vacuum freeze drying, ginsenoside Rd12 powders were dissolved in deuterated methanol. 1D NMR and 2D NMR spectroscopies of ginsenoside Rd12 were recorded on an Advance DMX-600 NMR spectrometer (Bruker, Karlsruhe, Germany).

## 4. Conclusions

In summary, Bs-YjiC from *B. subtilis* 168 was demonstrated to be a robust UGT, which can effectively and selectively glucosylate the C12 hydroxyl group of ginsenoside Rg3 to synthesize an unnatural ginsenoside Rd12 for the first time. Our studies revealed that unnatural ginsenoside Rd12 exhibited better solubility and stronger cytotoxicity against diverse cancer cell lines than those of ginsenoside Rg3. The in vivo and in vitro pharmacological activities of unnatural ginsenoside Rd12 should be further investigated.

**Supplementary Materials:** The following are available online at [www.mdpi.com/xxx/s1](http://www.mdpi.com/xxx/s1). Figure S1,  $^1\text{H}$  NMR of ginsenoside Rd12; Figure S2,  $^{13}\text{C}$  NMR of ginsenoside Rd12; Figure S3, HMBC spectra of ginsenoside Rd12; Figure S4, HSQC spectra of ginsenoside Rd12; Figure S5, COSY spectra of ginsenoside Rd12; Figure S6, Kinetic analysis of Bs-YjiC toward ginsenoside Rg3.

**Author Contributions:** Conceptualization, Y.H. and L.D.; methodology, H.L. and Y.Q.; validation, Y.Q. and X.Z.; formal analysis, Y.H. and H.Z.; data curation, Y.H.; writing—original draft preparation, Y.H.; writing—review and editing, J.Z. and L.D.; funding acquisition, L.D. All authors have read and agreed to the published version of the manuscript.

**Funding:** This research was supported by the National Natural Science Foundation of China (No. 21702226), China Postdoctoral Science Foundation (No. 2019M662575), and Hubei Postdoctoral Sustentation Foundation.

**Conflicts of Interest:** The authors declare no conflict of interest.

## References

- Kim, S.-A.; Shin, K.-C.; Oh, D.-K. Complete biotransformation of protopanaxadiol-type ginsenosides into 20-O- $\beta$ -glucopyranosyl-20(S)-protopanaxadiol by permeabilized recombinant *Escherichia coli* cells coexpressing  $\beta$ -glucosidase and chaperone genes. *J. Agric. Food Chem.* **2019**, *67*, 8393–8401.
- Wan, X.; Ren, Y.; Sun, X.; Liu, S. Classification and analysis of set prescription preparations containing *Panax ginseng* in 2015 edition of Chinese Pharmacopoeia (Part I). *China Pharm.* **2018**, *29*, 69–73.
- Leung, K.W.; Wong, A.S. Ginseng and male reproductive function. *Spermatogenesis* **2013**, *3*, e26391.
- Han, J.-Y.; Kim, H.-J.; Kwon, Y.-S.; Choi, Y.-E. The Cyt P450 enzyme CYP716A47 catalyzes the formation of protopanaxadiol from dammarenediol-II during ginsenoside biosynthesis in *Panax ginseng*. *Plant Cell Physiol.* **2011**, *52*, 2062–2073.
- Seki, H.; Tamura, K.; Muranaka, T. P450s and UGTs: Key players in the structural diversity of triterpenoid saponins. *Plant Cell Physiol.* **2015**, *56*, 1463–1471.
- Yu, T.; Yang, Y.; Kwak, Y.-S.; Song, G.G.; Kim, M.-Y.; Rhee, M.H.; Cho, J.Y. Ginsenoside Rc from *Panax ginseng* exerts anti-inflammatory activity by targeting TANK-binding kinase 1/interferon regulatory factor-3 and p38/ATF-2. *J. Ginseng Res.* **2017**, *41*, 127–133.
- Ahuja, A.; Kim, J.H.; Kim, J.-H.; Yi, Y.-S.; Cho, J.Y. Functional role of ginseng-derived compounds in cancer. *J. Ginseng Res.* **2018**, *42*, 248–254.
- Peng, D.; Chen, W.; Xie, J. Antihyperglycemic effects of ginseng and possible mechanisms. *Drugs Future* **2008**, *33*, 507–514.
- Tan, B.K.; Vanitha, J. Immunomodulatory and antimicrobial effects of some traditional Chinese medicinal herbs: A review. *Curr. Med. Chem.* **2004**, *11*, 1423–1430.
- Dai, L.; Li, J.; Yang, J.; Zhu, Y.; Men, Y.; Zeng, Y.; Cai, Y.; Dong, C.; Dai, Z.; Zhang, X. Use of a promiscuous glycosyltransferase from *Bacillus subtilis* 168 for the enzymatic synthesis of novel protopanaxatriol-type ginsenosides. *J. Agric. Food Chem.* **2018**, *66*, 943–949.
- Wei, W.; Wang, P.; Wei, Y.; Liu, Q.; Yang, C.; Zhao, G.; Yue, J.; Yan, X.; Zhou, Z. Characterization of *Panax ginseng* UDP-glycosyltransferases catalyzing protopanaxatriol and biosyntheses of bioactive ginsenosides F1 and Rh1 in metabolically engineered yeasts. *Mol. Plant* **2015**, *8*, 1412–1424.
- Yan, X.; Fan, Y.; Wei, W.; Wang, P.; Liu, Q.; Wei, Y.; Zhang, L.; Zhao, G.; Yue, J.; Zhou, Z. Production of bioactive ginsenoside compound K in metabolically engineered yeast. *Cell Res.* **2014**, *24*, 770–773.
- Hu, Y.; Xue, J.; Min, J.; Qin, L.; Zhang, J.; Dai, L. Biocatalytic synthesis of ginsenoside Rh2 using *Arabidopsis thaliana* glucosyltransferase-catalyzed coupled reactions. *J. Biotechnol.* **2020**, *309*, 107–112.
- Gantt, R.W.; Goff, R.D.; Williams, G.J.; Thorson, J.S. Probing the aglycon promiscuity of an engineered glycosyltransferase. *Angew. Chem. Int. Ed.* **2008**, *47*, 8889–8892.
- Cheng, Y.; Zhang, J.; Shao, Y.; Xu, Y.; Ge, H.; Yu, B.; Wang, W. Enzyme-Catalyzed Glycosylation of Curcumin and Its Analogues by Glycosyltransferases from *Bacillus subtilis* ATCC 6633. *Catalysts* **2019**, *9*, 734.
- Pandey, R.P.; Bashyal, P.; Parajuli, P.; Yamaguchi, T.; Sohng, J.K. Two trifunctional leloir glycosyltransferases as biocatalysts for natural products glycodiversification. *Org. Lett.* **2019**, *21*, 8058–8064.
- Chiang, C.-M.; Wang, T.-Y.; Yang, S.-Y.; Wu, J.-Y.; Chang, T.-S. Production of new isoflavone glucosides from glycosylation of 8-hydroxydaidzein by glycosyltransferase from *Bacillus subtilis* ATCC 6633. *Catalysts* **2018**, *8*, 387.
- Hu, Y.M.; Min, J.; Qu, Y.Y.; Zhang, X.; Zhang, J.K.; Yu, X.J.; Dai, L.H. Biocatalytic synthesis of calycosin-7-O- $\beta$ -D-glucoside with UDP-glucose regeneration system. *Catalysts* **2020**, *10*, 258.
- Chang, T.-S.; Chiang, C.-M.; Kao, Y.-H.; Wu, J.-Y.; Wu, Y.-W.; Wang, T.-Y. A new triterpenoid glucoside from a novel acidic glycosylation of ganoderic acid a via recombinant glycosyltransferase of *Bacillus subtilis*. *Molecules* **2019**, *24*, 3457.

20. Pandey, R.P.; Li, T.F.; Kim, E.-H.; Yamaguchi, T.; Park, Y.I.; Kim, J.S.; Sohng, J.K. Enzymatic synthesis of novel phloretin glucosides. *Appl. Environ. Microbiol.* **2013**, *79*, 3516–3521.
21. Dai, L.; Li, J.; Yang, J.; Men, Y.; Zeng, Y.; Cai, Y.; Sun, Y. Enzymatic synthesis of novel glycyrrhizic acid glucosides using a promiscuous *Bacillus* glycosyltransferase. *Catalysts* **2018**, *8*, 615.
22. Dai, L.; Li, J.; Yao, P.; Zhu, Y.; Men, Y.; Zeng, Y.; Yang, J.; Sun, Y. Exploiting the aglycon promiscuity of glycosyltransferase Bs-YjiC from *Bacillus subtilis* and its application in synthesis of glycosides. *J. Biotechnol.* **2017**, *248*, 69–76.
23. Dai, L.; Liu, C.; Li, J.; Dong, C.; Yang, J.; Dai, Z.; Zhang, X.; Sun, Y. One-pot synthesis of ginsenoside Rh2 and bioactive unnatural ginsenoside by coupling promiscuous glycosyltransferase from *Bacillus subtilis* 168 to sucrose synthase. *J. Agric. Food Chem.* **2018**, *66*, 2830–2837.
24. Wang, P.; Wei, Y.; Fan, Y.; Liu, Q.; Wei, W.; Yang, C.; Zhang, L.; Zhao, G.; Yue, J.; Yan, X. Production of bioactive ginsenosides Rh2 and Rg3 by metabolically engineered yeasts. *Metab. Eng.* **2015**, *29*, 97–105.
25. Dai, L.; Liu, C.; Zhu, Y.; Zhang, J.; Men, Y.; Zeng, Y.; Sun, Y. Functional characterization of cucurbitadienol synthase and triterpene glycosyltransferase involved in biosynthesis of mogrosides from *Siraitia grosvenorii*. *Plant Cell Physiol.* **2015**, *56*, 1172–1182.
26. Wang, P.; Wei, W.; Ye, W.; Li, X.; Zhao, W.; Yang, C.; Li, C.; Yan, X.; Zhou, Z. Synthesizing ginsenoside Rh2 in *Saccharomyces cerevisiae* cell factory at high-efficiency. *Cell Discov.* **2019**, *5*, 1–14.
27. Lu, J.; Yao, L.; Li, J.-X.; Liu, S.-J.; Hu, Y.-Y.; Wang, S.-H.; Liang, W.-X.; Huang, L.-Q.; Dai, Y.-J.; Wang, J. Characterization of UDP-glycosyltransferase involved in biosynthesis of ginsenosides Rg1 and Rb1 and identification of critical conserved amino acid residues for its function. *J. Agric. Food Chem.* **2018**, *66*, 9446–9455.
28. Jung, S.-C.; Kim, W.; Park, S.C.; Jeong, J.; Park, M.K.; Lim, S.; Lee, Y.; Im, W.-T.; Lee, J.H.; Choi, G. Two ginseng UDP-glycosyltransferases synthesize ginsenoside Rg3 and Rd. *Plant Cell Physiol.* **2014**, *55*, 2177–2188.
29. Xie, K.; Dou, X.; Chen, R.; Chen, D.; Fang, C.; Xiao, Z.; Dai, J. Two novel fungal phenolic UDP glycosyltransferases from *Absidia coerulea* and *Rhizopus japonicus*. *Appl. Environ. Microbiol.* **2017**, *83*, e03103–e03116.
30. Zhou, M.; Hou, Y.; Hamza, A.; Zhan, C.-G.; Bugni, T.S.; Thorson, J.S. Probing the regiospecificity of enzyme-catalyzed steroid glycosylation. *Org. Lett.* **2012**, *14*, 5424–5427.
31. Lepak, A.; Gutmann, A.; Kulmer, S.T.; Nidetzky, B. Creating a water-soluble resveratrol-based antioxidant by site-selective enzymatic glucosylation. *ChemBioChem* **2015**, *16*, 1870–1874.



© 2020 by the authors. Licensee MDPI, Basel, Switzerland. This article is an open access article distributed under the terms and conditions of the Creative Commons Attribution (CC BY) license (<http://creativecommons.org/licenses/by/4.0/>).